

Investigation of Switching Time in GaN/AIN Resonant Tunneling Diodes by Experiments and P-SPICE Models

W.-D. Zhang[®], Senior Member, IEEE, T. A. Growden[®], D. F. Storm, D. J. Meyer[®], Senior Member, IEEE, P. R. Berger, Fellow, IEEE, and E. R. Brown, Fellow, IEEE

Abstract—The experimental and simulated switching behavior across the negative differential resistance (NDR) region of GaN/AIN double-barrier resonant tunneling diodes (RTDs) is presented. The shortest 10%–90% experimental switching time was $\sim\!55$ ps. The experimental results are also studied with P-SPICE circuit models, which show that the relatively low peak-to-valley current ratio ($\sim\!1.5$), relatively high specific contact resistance ($\geq\!1\times10^{-6}~\Omega\text{-cm}^2$), and relatively large specific capacitance limit the switching time.

Index Terms—GaN/AIN, heterostructure, measurement, modeling, P-SPICE, resonant tunneling diode (RTD), switching time.

I. INTRODUCTION

aN-BASED heterostructures have broad applications, with notable examples being FETs [1] and light-emitting devices [2]. These successes and the large-band offset have motivated researchers to begin the exploration of vertical GaN-based heterostructures as a platform for other types of devices. Recently, GaN/AlN/GaN resonant tunneling diodes (RTDs) have demonstrated highly repeatable operation at room temperature while suffering no obvious degradation from traps. This success is attributable to better design methodology that addresses the high polarization fields, high-quality homoepitaxial growth methods, and improved fabrication techniques

Manuscript received September 1, 2019; revised October 22, 2019; accepted November 18, 2019. Date of publication December 16, 2019; date of current version December 30, 2019. This work was supported in part by the U.S. Office of Naval Research through the Devices and Architectures for THz Electronics (DATE) Multidisciplinary University Research Initiative (MURI) (program manager Dr. P. Maki) under Grant N00014-11-1-0721, in part by the Naval Research Laboratory (NRL) Base program, and in part by the National Science Foundation (program director Dr. D. Pavlidis) under Grant 1711733 and Grant 1711738. The review of this article was arranged by Editor P. J. Fay. (Corresponding author: W.-D. Zhang.)

W.-D. Zhang and E. R. Brown are with the Department of Physics, Wright State University, Dayton, OH 45435 USA, and also with the Department of Electrical Engineering, Wright State University, Dayton, OH 45435 USA (e-mail: wzzhang@fastmail.fm; elliott.brown@wright.edu).

T. A. Growden was with the Department of Electrical and Computer Engineering, The Ohio State University, Columbus, OH 43210 USA. He is now with the Naval Research Laboratory, Washington, DC 20375 USA. D. F. Storm and D. J. Meyer are with the U.S. Naval Research

Laboratory, Washington, DC 20375 USA.

P. R. Berger is with the Department of Electrical and Computer

Engineering, The Ohio State University, Columbus, OH 43210 USA. Color versions of one or more of the figures in this article are available online at http://ieeexplore.ieee.org.

Digital Object Identifier 10.1109/TED.2019.2955360

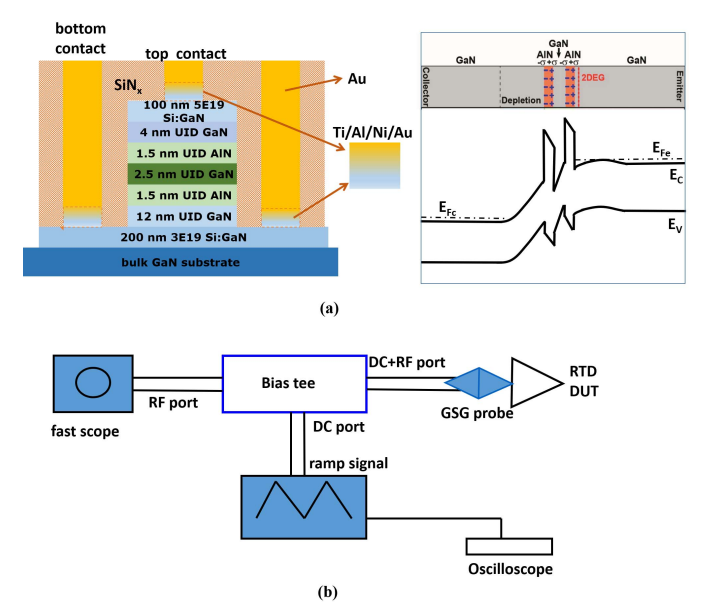


Fig. 1. (a) Left: GaN/AIN heterostructure stack used for the fabrication of GaN/AIN RTDs. Right: band diagram of the heterostructure under a 5-V bias. (b) Experimental setup for switching time measurements.

[3], [4]. However, questions remain on whether GaN/AlN RTDs are capable of being implemented as oscillators and switches with speeds that can compete with earlier RTDs based on GaAs/AlGaAs, InGaAs/AlAs, and InAs/AlSb materials despite the recent progresses such as the one reported in [5]. The wide-bandgap and the excellent thermal conductivity of GaN allow very high current density and high-voltage operation of RTDs [6], but can these merits provide any advantages for GaN-based RTDs in high-speed applications? This article reports our latest investigation into this issue, specifically the first switching time measurements on GaN/AlN RTDs. In addition, we have conducted P-SPICE simulations to better explain the measured data. Together, the experiments and the models presented here provide insight for designing the next-generation high-speed, high-voltage, and high-power GaN/AlN RTDs.

II. SWITCHING TIME MEASUREMENTS

The GaN/AlN/GaN RTD heterostructure studied in this article is shown in Fig. 1(a). Its growth and fabrication have been described in detail elsewhere [3], [7]. Fig. 1(b) shows

0018-9383 © 2019 IEEE. Personal use is permitted, but republication/redistribution requires IEEE permission. See http://www.ieee.org/publications_standards/publications/rights/index.html for more information.

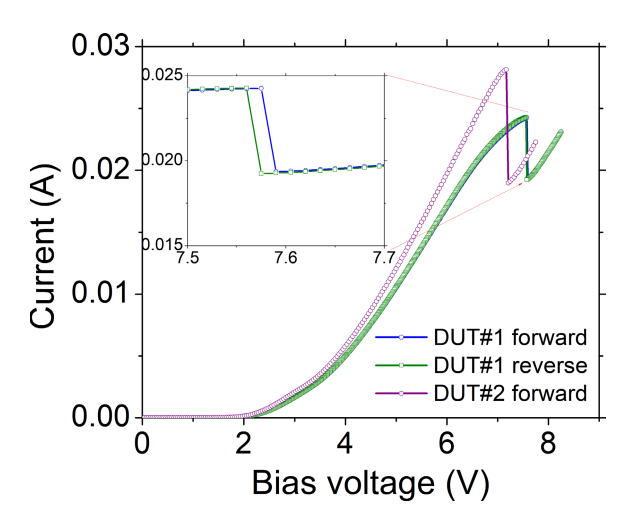


Fig. 2. *I–V* characteristics of GaN/AIN RTD #1 including both sweep and backward sweeps. The inset is a zoomed-in view of the NDR region, showing a hysteresis due to the effect of series resistance. The *I–V* characteristic of RTD #2 is also plotted.

the experimental setup, which was used to investigate the switching time of the GaN/AlN RTDs. The same setup was previously used to successfully measure the switching time of In_{0.53}Ga_{0.47}As/AlAs RTDs [8], [9]. At the center of the setup is an Anritsu bias tee with a rise time of $t_1 \sim 7$ ps. The dc port of the bias tee is connected to a ramp signal generator, which produces a dc offset bias along with a triangular waveform that triggers the switching events. The RF port of the bias tee is connected to a fast oscilloscope, in this case, an Infiniium MSOS804A 8-GHz oscilloscope, via a SubMiniature version A (SMA) coaxial cable. The Infiniium oscilloscope has an internal rise/fall time of $t_2 = 53.8$ ps [10], which needs to be deembedded from the total measured 10%-90% switching time. The dc + RF port of the bias tee is connected to a GaN/AlN RTD device under test (DUT). The dc offset ($V_{\rm dc}$) and the ramp signal $[V_{\text{ramp}}(t)]$ bias voltages are applied to the DUT via a ground-signal-ground (GSG) probe having a $200-\mu m$ pitch and a bandwidth of 40 GHz. The total voltage $V_{\rm dc} + V_{\rm ramp}(t)$ was monitored with a standard (low-speed) oscilloscope.

First, the I-V characteristics (i.e., I_M versus V_M) of the DUTs were taken with a Keithley 2400 source meter. For the first RTD (DUT #1), both forward and backward (voltage) sweeps were conducted. The plots are shown in Fig. 2, and the zoomed-in view of the negative differential resistance (NDR) region reveals a small hysteresis that is known to be associated with a significant series resistance R_s . Similar studies were performed on the second RTD device (DUT #2) from the same batch of devices. Its NDR region displays a small hysteresis too. Fig. 2 shows only the forward I-V plot of DUT #2, which will be studied in detail, as it has a higher peak-to-valley current ratio (PVCR). The I-V curve has a peak voltage of $V_P = 7.17 \text{ V}$ and a valley of $V_V = 7.21 \text{ V}$. The peak current is $I_P = 28.1$ mA, and the valley current is $I_V = 19.0$ mA. The corresponding PVCR is estimated to be \sim 1.48, which is much less than that of high-quality InGaAs/AlAs RTDs [8], but among the best performance of GaN/AlN RTDs reported

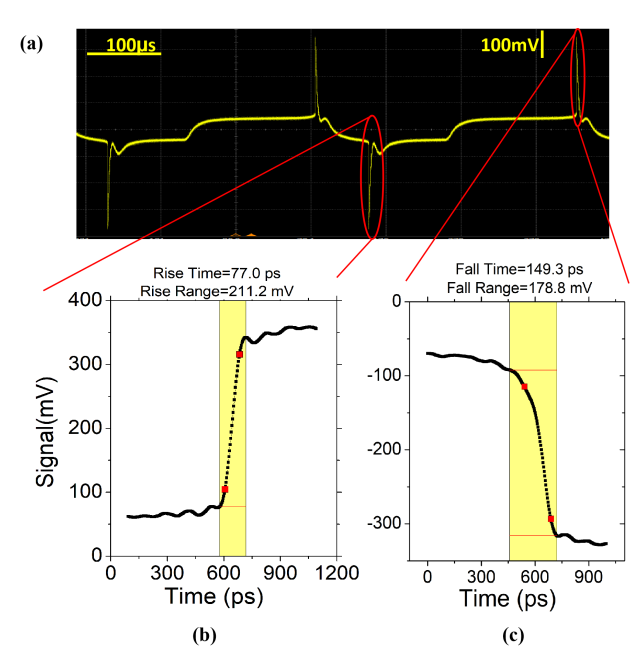


Fig. 3. (a) Voltage signal appeared on the Infiniium oscilloscope for the GaN RTD device #2 and the zoomed-in view of the switching events. The frequency of the ramp signal was set at 3 kHz. (b) Rise-time measurement of the GaN/AIN RTD by zooming-in the (front) edge of the spike, which is marked with the red cycle. Note that the polarity of the voltage signal is reversed. (c) Fall-time measurement.

in the literature so far. As shown later, a high PVCR is desired because it supports faster switching time.

From the I-V curve of DUT #2, the negative resistance across the NDR region $R_{\rm NDR} = (V_V - V_P)/(I_V - I_P)$ is estimated to be $R_{\rm NDR} \approx -4.2~\Omega$. To induce switching events, the maximum of the voltage signal $[V_{\rm dc} + V_{\rm ramp}(t)]$ was tuned to be greater than V_V , while the minimum was adjusted lower than V_P . No self-oscillation from the NDR, which could derail switching events, was observed.

Fig. 3(a) shows the screenshot of the switching events of DUT #2 on a 100- μ s scale measured with the fast oscilloscope (e.g., the Infiniium). Note that the polarity of the measured voltage signal needs to be reversed to extract the rise time and the fall time. In other words, the downward and upward spikes exhibit the rise and fall switching events, respectively. Then, the edges of the spikes shown in Fig. 3(a) were amplified with a finer time resolution. The 10%–90% rise time was found to be $t_{\text{tot},r} \approx 77$ ps [see Fig. 3(b)], while the 10%–90% fall time was $t_{\text{tot},f} \approx 149$ ps [see Fig. 3(c)]. Measurements on DUT #1 and other devices from the same substrate produced similar results.

After subtraction of the oscilloscope's rise (fall) time as well as the bias tee's rise time through the relationship $(t_{\text{tot}}^2 - t_1^2 - t_2^2)^{1/2}$, the intrinsic 10%–90% rise time of the RTD switching is estimated to be $t_r \approx 55$ ps, and the intrinsic 10%–90% fall time is $t_f \approx 139$ ps. Noticeably, the rise time is shorter than the fall time. This is a behavior that has been observed previously in InGaAs/AlAs RTDs, which had a rise time of \sim 21 ps compared with a fall time of \sim 38 ps [8], [9]. Despite the fact that the measured switching time of these GaN/AlN RTDs is slower than that of InGaAs/AlAs RTDs,

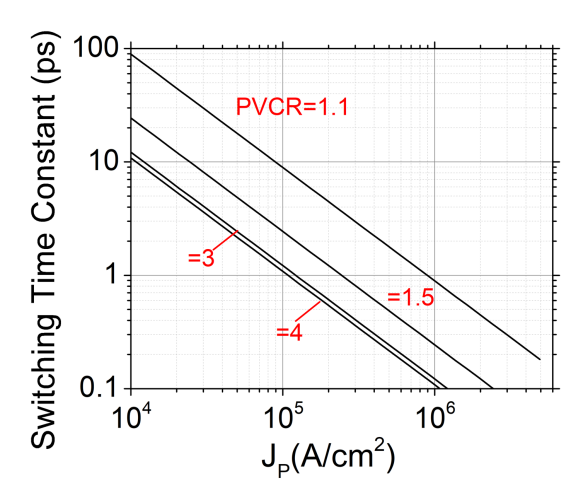


Fig. 4. Switching time versus peak current density.

this is the first direct measurement of the switching time in vertical GaN/AlN RTDs to the best of our knowledge and illustrates that the GaN/AlN RTDs are intrinsically capable of very high speeds.

Switching events in the GaN/AlN RTDs are complicated because the tunneling time through the AlN barriers and the dwell time in the GaN well are influenced by the polarization charge densities at the interfaces of the Wurtzite heterostructures [see Fig. 1(b)]. However, by analyzing the equivalent circuit of GaN/AlN RTDs, the 10%–90% time for a switching event from peak to valley can be still estimated with [11]

$$t_R \approx 4.4 \frac{\Delta V}{S} \tag{1}$$

which has been applied to InGaAs/AlAs RTDs previously. $S = \Delta J/C_A = (J_P - J_V)/C_A$ is called the speed index. $\Delta V = V_V - V_P$ is the voltage span of the NDR region. $\Delta J = J_P - J_V$ is the current span of the NDR region, where J_P and J_V are the peak and valley current densities, respectively. C_A is the specific capacitance with contributions from the accumulated emitter region, the barrier-quantum-well-barrier region, and the depleted collector region, in kind. ΔV , ΔJ , and C all are phenomenal parameters, which depend on the intrinsic properties of the GaN/AlN devices. In principle, they can be determined with measurements. Note that S can also be written as a function of PVCR and J_P , $S = J_P(1 - 1/\text{PVCR})/C_A$, which indicates that a larger PVCR enables a faster device speed.

Because the capacitance of the RTD was difficult to measure experimentally, we estimated it by evaluating the space charge versus bias voltage spanning over the entire RTD structure with a Poisson solver provided by Silvaco ATLAS [13]. The significant effect from the polarization fields at the GaN/AIN heterointerfaces was taken into account, and from this calculation, the specific capacitance was found to be $C_A \approx 4.8 \text{ fF}/\mu\text{m}^2$. Given the device area of $A \approx 11 \mu\text{m}^2$, the capacitance for the RTD is $C = C_A A \approx 52.8 \text{ fF}$. Note that C_A may be underestimated, as this method leaves out the capacitance associated with the charging and discharging of the GaN quantum well during the transition from the positive differential region (PDR) to NDR and vice versa [see Fig. 1(a)] [12].

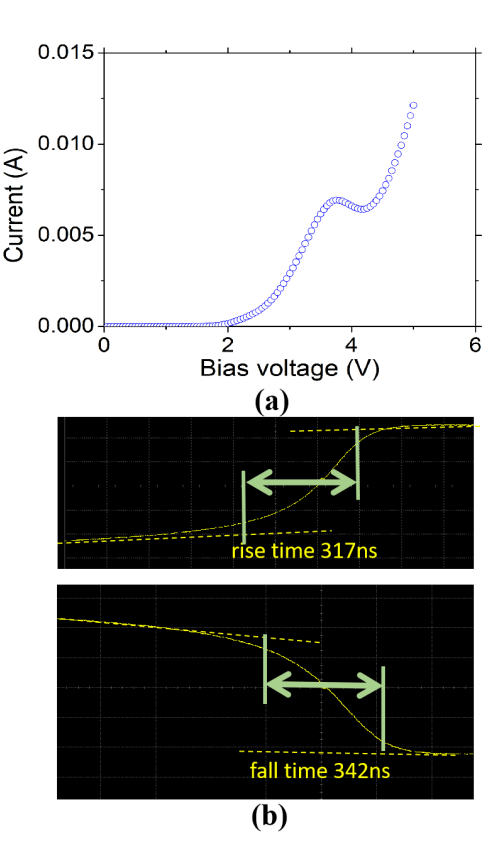


Fig. 5. (a) I-V curve of DUT #3. (b) Switching time measurement results.

The peak and valley current densities ($J_P = I_P/A$ and $J_V = I_V/A$) and their PVCR are easily evaluated from the I-V curve #2 shown in Fig. 2.

With the speed-index formula (1), the dependence of switching time t_R on J_P , as well as PVCR, was evaluated and shown in Fig. 4. Using the PVCR of \sim 1.4 and the peak current density of $J_P \sim 2.6 \times 10^5$ A/cm², we reached a theoretical value of $t_R \sim 1$ ps, which is significantly less than the experimental data.

Furthermore, we considered an opposite scenario by testing the third RTD device (DUT #3) but from a different substrate with a lower current density of $\sim 9.6 \times 10^3$ A/cm² and a smaller PVCR of ~ 1.1 [see Fig. 5(a)]. The 10%–90% rise time was measured to be ~ 317 ns, and the fall time was ~ 342 ns. Both were much longer than that of DUT #2, as expected [see Fig. 5(b)]. However, they are also significantly longer than ~ 90 ps predicted with Fig. 4.

Nevertheless, despite the quantitative differences, both the experimental and modeling results of DUT #1, #2, and #3 confirm that high-speed switching can be achieved in those devices with large PVCRs and high peak current densities.

III. P-SPICE MODELS FOR GAN/ALN RTDS

To gain a better understanding of the discrepancy between the experimental data and the modeling results of (1), we performed P-SPICE simulations on an equivalent circuit for RTDs, which is shown in Fig. 6. The RTD is modeled as an ideal diode, which is shown inside the dashed box of Fig. 6, along with several lumped elements: C and R_s , where C is the capacitance and R_s is the series resistance. We make the

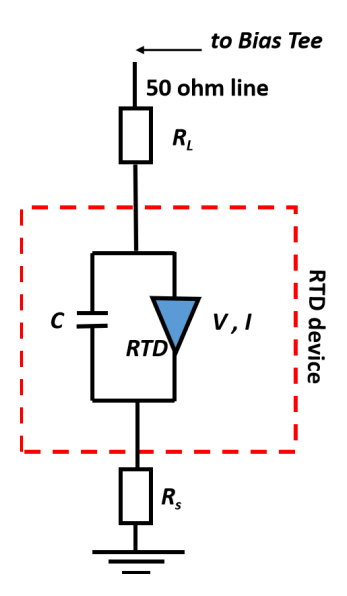


Fig. 6. Circuit model for GaN/AIN RTD devices used in P-SPICE simulations.

assumption that R_s is mostly contact resistance. R_L is load-line resistance.

The ideal diode has an I-V characteristic that can be described by the following equation [14], [15]:

$$I = C_1 V^i \{ \tan^{-1} [C_2 (V - V_T)] - \tan^{-1} [C_2 (V - V_N)] \}$$

+ $C_3 V^j + C_4 V^k$ (2)

where C_1 , C_2 , C_3 , and C_4 are numerical constants. V_T is defined as the threshold voltage where the second-order derivative d^2I/dV^2 has a local maximum. V_N is defined as the bias in the NDR region where the current variation is the steepest. i, j, and k are integer exponents ≥ 2 .

Their values were set as i = 3, j = 5, and k = 3, the same as in the modeling of InGaAs/AlAs RTDs [12]. The rest of the parameters of (2) are obtained by fitting the I-V curve of the ideal RTD diode, which is corrected by subtracting the voltage drop across the series resistance R_s from the experimental I-V curve through Kirchhoff's law

$$V = V_M - I_M R_s \tag{3}$$

$$I = I_M \tag{4}$$

where V_M and I_M are the measured voltage and current shown in Fig. 2. This correction is necessary based upon the analysis that a tiny hysteresis loop appears on forward and backward sweeps because of series resistance. The value of R_s is estimated in the range of 50–75 Ω (corresponding to $\sim 5.5-8.3 \times 10^{-6} \Omega \cdot \text{cm}^2$) by adjusting the value of R_s until the hysteresis begins to disappear on the corrected I-V curves of Fig. 2.

The circuit model of Fig. 6 was implemented in a schematic in P-SPICE along with a script programmed for (2) [16]. A sinusoidal waveform was selected to mimic the triangular ramp signal used in the experiments because it is easier to be realized in the software. Fig. 7(a) shows a P-SPICE simulation with the following parameters: $V_{\rm dc} = 6.5$ V, $V_{\rm ramp} = 3$ V, $R_s = 50$ Ω , and $R_L = 50$ Ω . The transient resolution

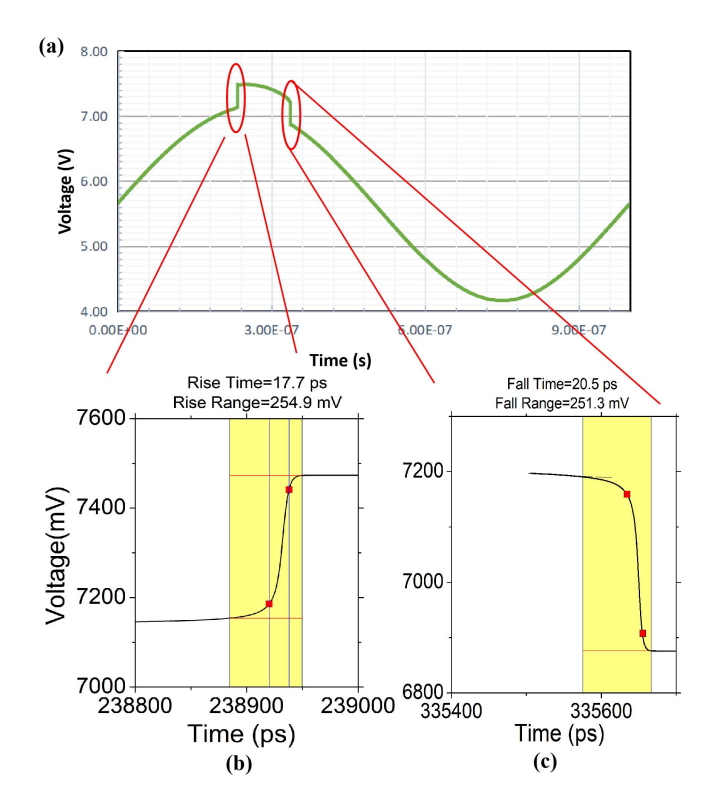


Fig. 7. (a) Simulation of a switching event with the P-SPICE models. (b) Zoomed-in view of the rise time. (c) Zoomed-in view of the fall time.

was set to 1 ps in order to evaluate accurately the switching time while maintaining acceptable computing time. As shown in Fig. 7(a), the switching behavior of both rising and falling events is reproduced by the simulation. From the zoomed-in view of Fig. 7(a), the 10%-90% rise time is estimated to be ~ 19 ps, while the fall time is ~ 23 ps. Both are shorter than the experimental values [see Fig. 7(b) and (c)].

Next, we studied the influence of R_s on t_R by treating it as a variable. The results are shown in Fig. 8(a). The plot confirms that a large R_s value indeed could slow down the switching speeds. And R_s may be responsible for why the rise time is the shorter one compared with the fall time in both GaN/AIN and InGaAs/AIAs RTDs. On the other hand, surprisingly, the R_s -dependence is not monotonic. The switching time t_R becomes shorter once the value of R_s is greater than 50 Ω , for example, $R_s = 75 \Omega$. This is likely caused by an increase of the NDR voltage span $\Delta V = \Delta I \times R_s$, which would reduce t_R according to (1).

In our GaN-based devices, both the top and bottom contacts were a Ti/Al/Ni/Au stack (see Fig. 1). With this type of ohmic contact stack, the minimum specific contact resistance (the best) obtained so far from the TLM structure data was $\sim 1 \times 10^{-6} \Omega$ -cm², from which the smallest R_s value was estimated to be $\sim 9.1 \Omega$. This corresponds to a rise time of ~ 6.2 ps according to Fig. 8(a). Thus, reducing the contact resistance is critical to accelerate future switching speeds, which may be achieved in two ways: 1) to optimize the ohmic metal stack and/or 2) to increase the thickness of metal films.

Another factor likely contributing to the difference between the experimental data and the SPICE models is the capacitance

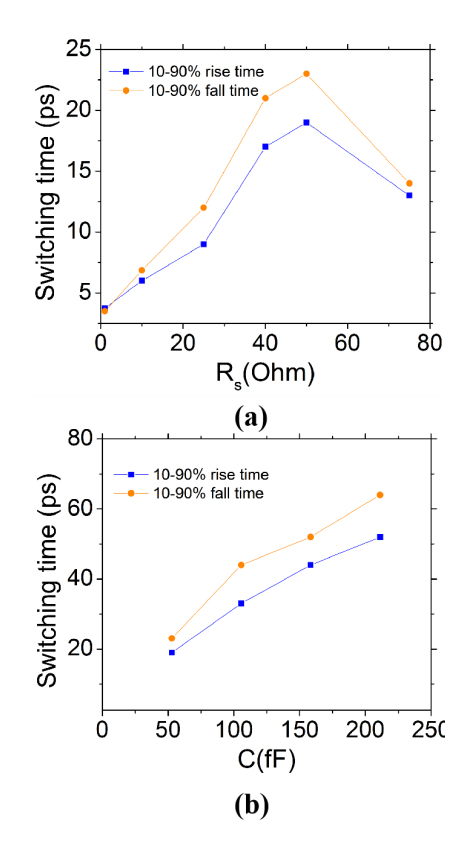


Fig. 8. Simulation on the influence of (a) $R_{\rm S}$ on 10%–90% switching time and (b) C.

C, which may be underestimated in the Silvaco calculations. As mentioned earlier, the capacitance resulted from the charging and discharging of the GaN quantum well is not included. This may add significant error to the estimation of the capacitance in the NDR region [12]. There are other possibilities. The actual area ($A_{\rm act}$) for the GaN/AlN stack could be greater than the one designed for the device ($A \approx 11~\mu {\rm m}^2$), which was used in the capacitor calculation. The fringe effect in the capacitor and the isolating Si₃N₄ region sandwiched between the GaN/AlN stack structure and the bottom contact may contribute additional unaccounted capacitance [see Fig. 1(a)].

Therefore, we investigated the C dependence of the switching time following the same procedure above. The results are shown in Fig. 8(b). As expected, the switching time becomes longer as the capacitance increases. If the capacitance is set to $C \sim 211$ fF, and the series resistance R_s is set to 50Ω , the rise time is ~ 54 ps, which is close to the experimental data.

IV. CONCLUSION

We measured the 10%–90% switching time of GaN/AlN RTDs and conducted detailed modeling with a speed-index formula as well as P-SPICE models. While the \sim 55-ps switching time (peak-to-valley) is slower than that reported in InGaAs/AlAs RTDs (i.e., \sim 21 ps), our results show great promise for GaN/AlN RTDs as high-speed, high-power oscillators.

The speed-index formula indicates that short switching time is correlated with high peak current densities and large PVCRs. This has been confirmed by the experiments. However, there is a significant discrepancy between the model and the

experimental data remaining to be explained. This is different from the previous studies on InGaAs/AlAs RTDs, where the speed-index formula easily gave a satisfied agreement with the experimental data [7].

The P-SPICE analysis reveals that the series resistance—mostly from the contacts of the devices—is an important factor contributing to this discrepancy, and it explains why the fall time is longer than the rise time. The series resistance could adversarially diminish the NDR voltage span, which is important to high-speed and high-power output. Thus, to obtain shorter switching time, it is worth putting effort into reducing contact resistances in GaN/AlN RTDs. The greater specific capacitance than the self-consistent Sivaco calculations could be another factor slowing down the switching speed of GaN/AlN RTDs. The enhancement is likely due to the quantum well capacitance in the NDR region, which is further complicated by the polarization effect in the Wurtzite GaN/AlN heterostructures. This is being investigated and will be presented in a future publication.

REFERENCES

- [1] O. Ambacher *et al.*, "Two dimensional electron gases induced by spontaneous and piezoelectric polarization in undoped and doped AlGaN/GaN heterostructures," *J. Appl. Phys.*, vol. 87, no. 1, pp. 334–344, 2000.
- [2] S. Nakamura, T. Mukai, and M. Senoh, "High-power GaN p-n junction blue-light-emitting diodes," *Jpn. J. Appl. Phys.*, vol. 30, no. 12A, 1991, Art. no. L1998.
- [3] T. A. Growden, D. F. Storm, W. Zhang, E. R. Brown, D. J. Meyer, P. Fakhimi, and P. R. Berger, "Highly repeatable room temperature negative differential resistance in AlN/GaN resonant tunneling diodes grown by molecular beam epitaxy," *Appl. Phys. Lett.*, vol. 109, no. 8, 2016, Art. no. 083504.
- [4] J. Encomendero et al., "New tunneling features in polar III-nitride resonant tunneling diodes," *Phys. Rev. X*, vol. 7, Oct. 2017, Art. no. 041017.
- [5] J. Encomendero et al., "Room temperature microwave oscillations in GaN/AlN resonant tunneling diodes with peak current densities up to 220 kA/cm²," Appl. Phys. Lett., vol. 112, Jan. 2018, Art. no. 103101.
- [6] T. A. Growden et al., "431 kA/cm² peak tunneling current density in GaN/AlN resonant tunneling diodes," Appl. Phys. Lett., vol. 112, Jan. 2018, Art. no. 033508.
- [7] D. F. Storm et al., "AlN/GaN/AlN resonant tunneling diodes grown by RF-plasma assisted molecular beam epitaxy on freestanding GaN," J. Vac. Sci. Technol. B, vol. 35, no. 2, 2017, Art. no. 02B110.
- [8] T. A. Growden, E. R. Brown, W. Zhang, R. Droopad, and P. R. Berger, "Experimental determination of quantum-well lifetime effect on largesignal resonant tunneling diode switching time," *Appl. Phys. Lett.*, vol. 107, Oct. 2015, Art. no. 153506.
- [9] W.-D. Zhang, E. R. Brown, T. A. Growden, P. R. Berger, and R. Droopad, "A nonlinear circuit simulation of switching process in resonant-tunneling diodes," *IEEE Trans. Electron Devices*, vol. 63, no. 12, pp. 4993–4997, Dec. 2016.
- [10] (2019). Keysight. [Online]. Available: https://literature.cdn.keysight.com/litweb/pdf/5991-3904EN.pdf?id=2447379
- [11] E. R. Brown, N. G. Einspruch, and W. R. Frensley, *Heterostructures and Quantum Devices*, N. G. Einspruch and W. R. Frensley, Eds. Orlando, FL, USA: Academic, 1994, p. 306.
- [12] N. Shimizu, T. Waho, and T. Ishibashi, "Capacitance anomaly in the negative differential resistance region of resonant tunneling diodes," *Jpn. J. Appl. Phys.*, vol. 36, no. 3B, pp. L330–L333, 1997.
- [13] (2016). Silvaco ATLAS. [Online]. Available: https://www.silvaco.com
- [14] E. R. Brown, O. B. McMahon, L. J. Mahoney, and K. M. Molvar, "SPICE model of the resonant-tunnelling diode," *Electron. Lett.*, vol. 32, pp. 938–940, May 1996.
- [15] E. R. Brown, W. D. Goodhue, and T. C. G. Sollner, "Fundamental oscillations up to 200 GHz in resonant tunneling diodes and new estimates of their maximum oscillation frequency from stationary-state tunneling theory," *J. Appl. Phys.*, vol. 64, pp. 1519–1529, Apr. 1988.
- [16] (2019). PSPICE. [Online]. Available: https://www.orcad.com/products/ orcad-pspice-designer/overview